European Polymer Journal 49 (2013) 3089–3094

Contents lists available at SciVerse ScienceDirect

European Polymer Journal

journal homepage: www.elsevier.com/locate/europolj

Macromolecular Nanotechnolgy

Hardness evaluation of cured urea–formaldehyde resins with different formaldehyde/urea mole ratios using nanoindentation method

Byung-Dae Park [a,*], Charles R. Frihart [b], Yan Yu [c], Adya P. Singh [a]

[a] Department of Wood Science and Technology, Kyungpook National University, Daegu 702-701, Republic of Korea
[b] Forest Products Laboratory, One Gifford Pinchot Drive, Madison, WI 53726, USA
[c] International Center for Bamboo and Rattan, Beijing 100102, China

ARTICLE INFO

Article history:
Received 16 March 2013
Received in revised form 29 May 2013
Accepted 5 June 2013
Available online 28 June 2013

Keywords:
Urea–formaldehyde resin
Hardness
Modulus
Nanoindentation
Crystal structure

ABSTRACT

To understand the influence of formaldehyde/urea (F/U) mole ratio on the properties of urea–formaldehyde (UF) resins, this study investigated hardness of cured UF resins with different F/U mole ratios using a nanoindentation method. The traditional Brinell hardness (H_B) method was also used for comparison. The H_B of cured UF resin films with different F/U mole ratios was determined after exposing the films to different post-curing temperatures. The nanoindentation method was employed for these films to measure Meyer hardness (H_M) and reduced modulus (E_r) which have been used to calculate the elastic modulus (E_s) of cured UF resins. As the F/U mole ratio decreased, the H_B decreased continuously, indicating a less rigid network structure in low F/U mole ratio UF resins. The higher the post-curing temperature, the greater the value of H_B. The H_M value also showed a similar trend as a function of F/U mole ratio. However, the E_r and E_s did not show a consistent trend as exhibited by H_M and H_B. Both H_M and E_r showed much greater variation in the coefficient of variation (COV) at lower F/U mole ratios 1.0 and 1.2, indicating a more heterogeneous composition of these resins. Linear relationships between H_M and E_r indicate that heterogeneity of the surface composition of samples contributes greatly to variations in the measured values. This variability is discussed in terms of crystal structures present in the cured UF resins of low F/U mole ratios.

1. Introduction

Urea–formaldehyde (UF) resin is one of the most important resins among formaldehyde-based resins, which include melamine–urea–formaldehyde (MUF) resin, melamine–formaldehyde (MF) resin, and phenol–formaldehyde (PF) resin. As a polymer formed by chemical reactions between formaldehyde and urea, UF resins are widely used as adhesive in the manufacture of wood-based composite panels, such as interior plywood, particleboard and medium density fiberboard with the wood-based panel industry being a major consumer of this type of resin.

While UF resins are valuable as lower cost, fast curing, good performance adhesives, which are also water soluble and colorless, formaldehyde emission (FE) from the panels is a critical disadvantage of this type of resin. The FE results primarily from UF resins in wood-based composite panels [1]. Furthermore, FE from the panels used for interior applications is a serious health concern, in that it has been related to sick building syndrome in an indoor environment. However, concerted and dedicated efforts are being made to reduce or control the FE from UF resin-bonded panels through developments in resin technologies [2–10].

* Corresponding author. Tel.: +82 53 950 5797; fax: +82 53 950 6751.
E-mail address: byungdae@knu.ac.kr (B.-D. Park).

0014-3057/$ - see front matter © 2013 Elsevier Ltd. All rights reserved.
http://dx.doi.org/10.1016/j.eurpolymj.2013.06.013

Among the methods attempted to reduce the FE, lowering of formaldehyde to urea (*F*/*U*) mole ratio for the synthesis of UF resins has been proved to be a very practical approach [8], and lower *F*/*U* molar ratios below 1.0 are being employed for UF resin synthesis these days. However, reduction achieved in the FE from UF resins with low *F*/*U* mole ratios has been at the expense of some important panel properties, such as bending strength, internal bond (IB) strength, thickness swelling, or water absorption by wood-based panels. For example, an excellent literature review on the influence of *F*/*U* mole ratio on the FE as well as panel properties was undertaken by Myers [3], and the information provided suggests that gel time used as an indicator of resin reactivity increased with decreasing *F*/*U* mole ratio. In general, lower *F*/*U* mole ratios cause less FE from panels, but with a loss in some panel properties, particularly IB strength and thickness swelling after water immersion for 24 h. Lower *F*/*U* mole ratios also reduced modulus of rupture (MOR) [8]. Lower cross-linking density of low *F*/*U* mole ratio UF resins compared to high *F*/*U* mole ratio UF resins [11] may be the reason for a reduction in such properties. However, despite much work on the impact of low *F*/*U* mole ratio on the FE and properties of wood-based panels [12–16], it is still not fully understood why low *F*/*U* mole ratio resins result in poor properties of wood-based composite panels. Characterization of mechanical properties, such as hardness or stiffness of solid state cured UF resins, is a promising approach for seeking an answer.

In recent years several high resolution techniques, such as atomic force microscopy (AFM) combined with nanoindentation, electron microscopy, or X-ray diffraction have been employed for material characterization at nano-scale [17]. Among these, we think that a nanoindenation technique coupled with AFM can provide nano-scale information on hardness of materials, may offer an insight because comparative hardness or stiffness values of cured UF resin adhesive can be obtained at a very small scale by this technique.

Characterization of materials by nanoindentation (also called depth sensing indentation) is based on the use of rigid indenters, typically with diamond or diamond coated tips, and since its proposal in 1992 by Oliver and Pharr [18], it is increasingly attracting interest in characterizing mechanical properties of polymers [19–23] and thin polymer films [24,25] at nano-scale. Nanoindentation has also been effectively used to characterize mechanical properties, such as hardness and modulus of elasticity, of wood cell wall [26–29] and bamboo cell wall [30]. The use of nanoindentation in characterizing the properties of wood–adhesive bond lines [31–33] and wood coatings [34,35] further extends its application in materials research. Konnerth et al. [31] reported that the hardness of phenol–resorcinol–formaldehyde (PRF) resins at wood-adhesive bond lines was greater than that of wood cell wall, and the impression gained is that the nanoindentation technique can serve as a useful method to test the performance of adhesives themselves.

To the authors' knowledge, the hardness of cured UF resins has not been characterized before using the nanoindentation technique. Therefore, our work is the first to provide information on mechanical properties of cured UF resins by measuring their hardness and elastic modulus by nanoindentation. For comparison, a traditional method of Brinell hardness was also applied for these resins after post-cure treatment at different temperatures.

2. Experimental details

2.1. Materials

Both the urea and formalin (37%) used for the synthesis of UF resins were technical grade. Aqueous solutions of both formic acid (20 wt%) and sodium hydroxide (NaOH) (20 wt%) were used to adjust the pH level during UF resin synthesis. Aqueous solution (20 wt%) of ammonium chloride (NH_4Cl) was used as the hardener.

2.2. Preparation of UF resins and their properties

All UF resins used for this study were prepared in the laboratory, following traditional alkaline-acid two-step reaction. The formalin (405.8 g) was placed in the reactor and then the pH was adjusted to pH 7.8 with aqueous NaOH and then a defined amount of the first urea (151.7 g) was added at 1-min intervals. Temperature slowly increased by 1 °C/min. to 90 °C where the reaction was kept for 1 h. Then the acidic reaction was initiated by adding formic acid (20 wt% solution), and adjusting the pH to about 4.6, and the condensation reactions were carried out until the target viscosity of JK was reached as measured using a bubble viscometer (VG-9100, Gardner-Holdt Bubble Viscometer, USA). Final *F*/*U* mole ratios of UF resins were adjusted by adding different amounts of the second urea addition. The amounts of the second urea were 37.9 g, 65.0 g, 101.1 g, and 151.7 g for *F*/*U* mole ratio of 1.6, 1.4, 1.2, and 1.0, respectively. Then, the UF resin was cooled to room temperature, and subsequently the pH was adjusted to 8.0 by adding aqueous NaOH.

The non-volatile solids content was determined by measuring approximately 1 g of the liquid UF resin in a disposable aluminum dish and taking an accurate weight before and after drying in a convective oven at 105 °C for 3 h. The viscosity of the UF resin was measured at 25 °C by a cone-plate viscometer (DV-II+, Brookfield, US) with a No. 2 spindle at 60 rpm. The gel time of the UF resins was measured at 100 °C by a gel time meter (Davis Inotek Instrument, Charlotte, NC) by adding 3% ammonium chloride (20% aqueous solution) based on the resin solids (see Table 1).

2.3. Preparation of cured UF resin films

In order to measure properties of cured UF resins, first 0.1% ammonium chloride (20% aqueous solution) based on the resin solids was thoroughly mixed with the liquid UF resin synthesized. Then films were prepared by casting the mixed liquid UF resin between two glass slides with a gap of 2 mm as shown in Fig. 1. The liquid UF resin was cured at 60 °C for 24 h in a drying oven, and then the rig

Table 1
Properties of liquid UF resins of different *F*/*U* mole ratios.

F/*U* mole ratio	Non-volatile solids (%wt)	Viscosity (mPa s)	Gelation time (s)
1.6	52.53	327.3	51
1.4	54.12	276.0	72
1.2	54.92	250.7	168
1.0	57.58	248.0	201

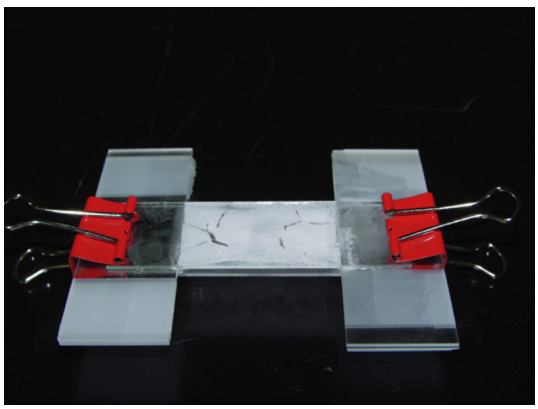

Fig. 1. A set-up rig for the film preparation of cured UF resin using glass slides.

was disassembled to remove the films which were used for the nanoindentation scan.

The film preparation conditions used in this work were somewhat different from those in industrial preparations of composites, because higher temperature employed for hot pressing in industrial operation resulted in broken pieces of cured UF resins. We optimized conditions so as to characterize cured UF resins without wood.

2.4. Measurements of mechanical properties of cured UF resin films

The cured UF resin films were exposed to different post-curing temperatures (100 °C, 110 °C, 120 °C and 130 °C) for 20 min in a drying oven and then used for the determination of Brinell hardness (H_B). The H_B values were measured using a 10 mm diameter (D) steel ball as an indenter (294N) attached to a universal testing machine (300TC, Hounsfield Test Equipment Ltd., Surry, England). The indentation depth (h) was set to equal to $1/\pi$ ($\fallingdotseq$0.32), where the force (P) was used to calculate the H_B by the Eq. (1) shown below:

$$H_B = \frac{P}{\pi D h} = \frac{P}{10} \tag{1}$$

In addition, the control film samples, which had not been post-cured, were also analyzed by nanoindenter equipped with a diamond Berkovich tip indenter (Tribo-indenter®, Hysitron, Minneapolis, Minnesota, USA) and AFM. The nanoindentation was replicated at least 30 indents per sample with a scanning area of 20 μm × 20 μm. All nanoindentation tests employed a three-segment load ramp in force control [18]. The Meyer hardness (H_M) was determined by the following equation:

$$H_M = \frac{L_{\max}}{A} \tag{2}$$

where $L_{\max}$ is the maximum load of the final partial unloading segment and A is the projected indent area at the $L_{\max}$.

Elastic punch theory states that the elastic modulus of materials and hardness can be inferred from load–displacement curves of nanoindentation. Fig. 2 displays a typical load–displacement curve of cured UF resin (*F*/*U* mole ratio of 1.2). The peak load and loading–unloading rates were 5000 μN/s and 50 μN/s for the indentation of samples. A load holding segment of 2 s was added between loading and unloading segments to remove the effect of creep. According to the method of Oliver and Pharr [18], the unloading segment can be fitted very well with a power-law function, from which the initial slope of the unloading curve, namely elastic contact stiffness (S) from load (L)–depth (h) curve, can be determined according to the Eq. (3). Based on the S, the reduced elastic modulus (E_r) can also be obtained by using the Eq. (4). The Er is termed because it takes into account the compliances of the indenter tip as shown by the Eq. (5). Then the elastic modulus (E_s) of samples can be calculated from the Eq. (5):

$$S = \frac{dL}{dh} = \frac{2}{\sqrt{\pi}} E_r \sqrt{A} \tag{3}$$

$$E_r = \frac{\sqrt{\pi}}{2} \frac{S}{\sqrt{A}} \tag{4}$$

$$\frac{1}{E_r} = \frac{1 - \nu_S^2}{E_S} + \frac{1 - \nu_i^2}{E_i} \tag{5}$$

Both E_i and ν_i are the elastic modulus and Poisson ratio of the tip. For diamond tips, E_i and ν_i are 1141 GPa and 0.07, respectively. For the calculation of cured UF resin films, the ν_s was assumed to be 0.45, used for phenol–resorcinol–formaldehyde (PRF) resin [32].

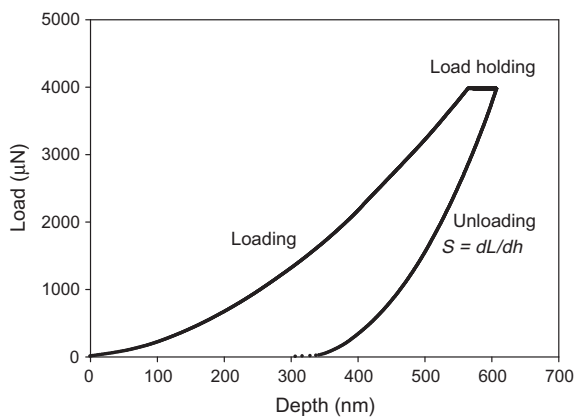

Fig. 2. A typical load–displacement curve of cured UF resin film (*F*/*U* mole ratio = 1.2).

3. Results and discussion

3.1. Brinell hardness of cured UF resins

Prior to undertaking nanoindentation work, traditional Brinell hardness (H_B) was measured for the cured UF resin films that were exposed to different temperatures as post-curing treatment. H_B values of cured UF resins as a function of F/U mole ratio and post-curing temperature are shown in Fig. 3. Both F/U mole ratio and post-cure temperature greatly impact the H_B values of cured UF resins. As expected, the H_B of cured UF resins decreased with lowering of F/U mole ratio from 1.6 to 1.0, while in comparison to control (i.e., no post-curing), it increased with an increase in the post-curing temperature. The highest H_B value of the cured UF resins was recorded for F/U mole ratio of 1.6 and the post-cure temperature of 130 °C, which also indicated a greater impact of F/U mole ratio than post-curing temperature to the H_B value. The results can be explained in terms of changes of either in cross-linking density or stiffness of cured UF resin as a function of F/U mole ratio. In other words, a decrease in the F/U mole ratio results in the reduction of branching in cured UF resins, and thus a decrease of cross-linking density and maximum storage modulus (E'_{max}), and an increase in the damping for cured UF resins of low F/U mole ratios [11]. It appears that an increase in the post-curing temperature also results in an increase in the cross-linking density of the resins of all F/U mole ratios.

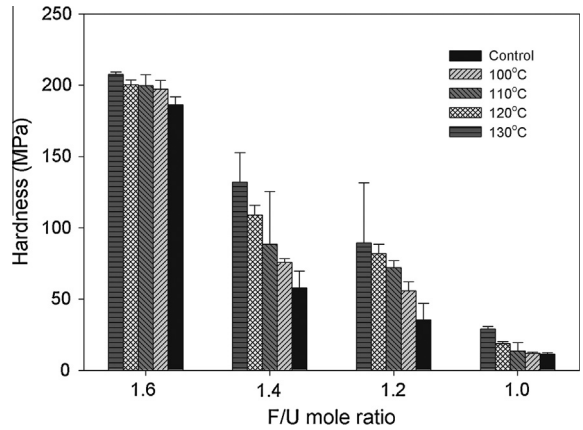

Fig. 3. H_B values of cured UF resin films at different F/U mole ratios and post-curing temperatures.

3.2. Hardness and modulus of cured UF resins by nanoindentation

Prior to measuring Meyer hardness (H_M) of cured UF resins using the nanoindentation method, the surface quality of cured UF resin films was evaluated. Fig. 4 shows typical surface images of cured UF resin films of F/U mole ratios of 1.0 and 1.6. The surface of cured UF resins of F/U mole ratio 1.0 (Fig. 4a) is considerably rougher compared to the surface of F/U mole ratio of 1.6. The pores present (blue[1] arrow in Fig. 4a) are considered to form from evaporation of water during curing of the resin by condensation reaction. In addition, irregular particles (white thick arrows in Fig. 4) were present on the surfaces of all F/U mole ratio samples, and are readily distinguishable from the indents produced by the three-sided indenter (black thick arrows in Fig. 4). The small particles may be what have been previously described as spherical structures [36,37]. Although some observations suggest that spherical particles are a feature only of UF resins of F/U mole ratios lower than 1.2 [38,39], we have recorded their presence also in higher mole ratio UF resins [36]. It has been considered that the crystallinity of cured UF resins may arise from such particles [40,41].

A relatively large indenter was used for all samples in this study because of variability in the quality of surface, with samples 1.0, 1.2, and 1.4 being much poorer that the sample of 1.6 F/U mole ratio. Field emission scanning electron microscope studies have shown these particles to be dispersed on the surfaces of all cured UF resin films, resulting in a heterogeneous composition of the resins regardless of F/U mole ratios, although fewer particles were present on the surfaces of high mole ratio resins compared to low mole ratio resins [36]. As will be discussed in greater detail later, we think that the surface quality of samples as related to surface roughness (Fig. 4) and the size and frequency of spherical particles [36], had an influence on the H_M and modulus values, measured by the nanoindentation.

Changes in the H_M values determined by the nanoindentation as a function of F/U mole ratio of cured UF resins are shown in Fig. 5. As expected from the H_B measurement, the H_M values decreased from 0.79 GPa to 0.57 GPa with a decrease in the F/U mole ratio from 1.6 to 1.0, and thus the results from nanoindentation measurements are consistent with those from H_B measurements. Lower H_M of low F/U mole ratio UF resins can be attributed to their lower cross-linking density and stiffness. In other words, cured UF resins increasingly become less hard as the cross-linking density decreases. In addition, the standard deviation of H_M measurements is increasingly larger as the F/U mole ratio decreases, and the poor surface quality of cured UF resins of low F/U mole ratio is likely to contribute to greater variation found in the measured values.

Changes in moduli, i.e., reduced modulus (E_r) and calculated elastic modulus (E_s) of cured UF resin film samples as a function of F/U mole ratio, are shown in Fig. 6. As the F/U mole ratio decreased, E_r value at first decreased at the F/U mole ratio of 1.4 and then increased up to 1.0 F/U mole ratio. E_s followed a trend similar to that for E_r, but with difference in the absolute values. Measured E_r values are greater than those of the E_s by an order of about 2 GPa. As shown in Eq. (5), the elastic modulus of the sample is calculated by incorporating the Poisson ratio of sample that was assumed as 0.45 from the reported literature [32]. Thus, the incorporation of the sample Poisson ratio into the Eq. (5) results in lower calculated elastic modulus compared to measured values for cured UF resins.

[1] For interpretation of color in Fig. 4, the reader is referred to the web version of this article.

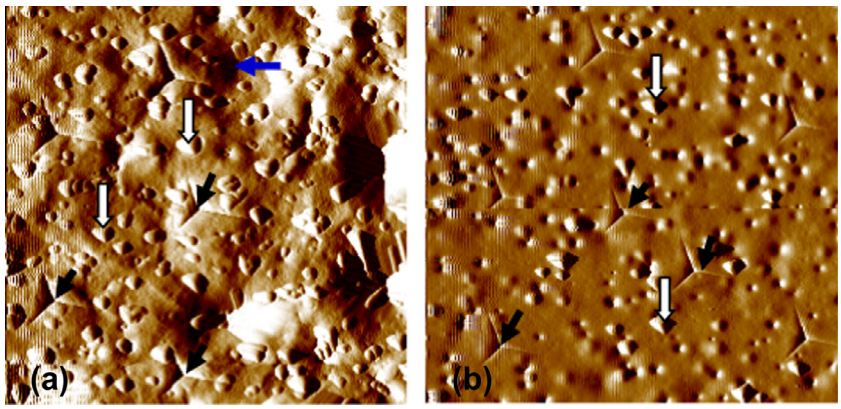

Fig. 4. Images of cured UF resin films after the nanoindentation, depending on the *F*/*U* mole ratio of (a) 1.0, and (b) 1.6.

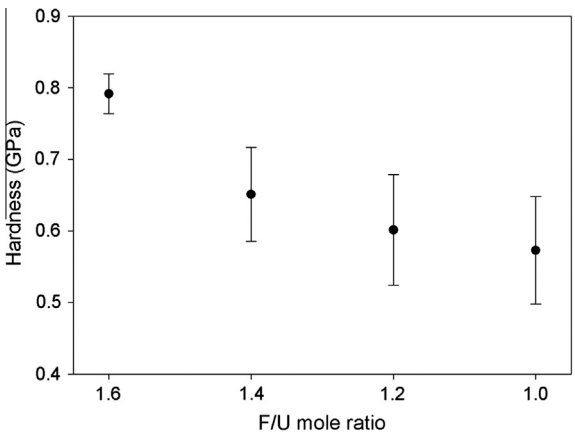

Fig. 5. Relationship of F/U mole ratio and the hardness (H_M) of cured UF resin films, measured by the nanoindentation.

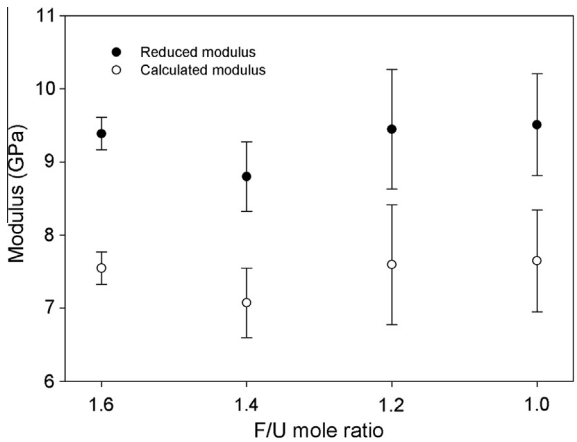

Fig. 6. E_r and E_s of cured UF resin films measured by the nanoindentation as a function of *F*/*U* mole ratio.

As indicated in Figs. 5 and 6, H_M, E_r and E_s values of cured UF resins of low *F*/*U* mole ratios of 1.2 and 1.0 showed greater variations with a relatively large standard deviation compared to those of higher *F*/*U* mole ratio resins. We made a quantitative comparison of the variation on the basis of the coefficient of variation (COV) as shown in Fig. 7. As expected, the COVs of both H_M and E_r gradually increased as the *F*/*U* mole decreased except for *F*/*U* mole ratio of 1.0, which showed less variation than *F*/*U* mole ratio of 1.2. Using field emission scanning electron microscopy (FE-SEM) in our earlier study two morphologically distinct phases were identifiable in the low mole ratio UF resins, crystalline and non-crystalline formations [35]. Crystalline aggregates were dispersed within the non-crystalline phase and were observable in fractured faces of resin films. The non-crystalline phase consisted of particles, predominantly of globular forms, within a less morphologically defined amorphous matrix [36]. Although reported lacking in previous studies [37], we found globular particles to be a component also of high mole ratio UF resins [36], although compared to low mole ratio UF resins globular particles were fewer and smaller. Greater variability in the modulus values of low mole ratio resins compared to

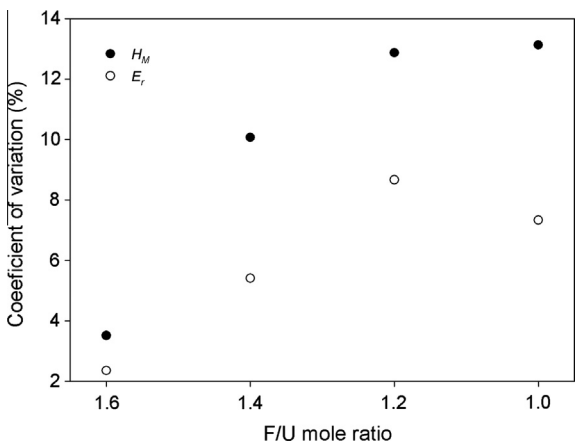

Fig. 7. Change of COV of both H_M and E_r of cured UF resin films, depending on the *F*/*U* mole ratio.

high mole ratio resins obtained using the nanoindentation method can be explained on the basis of above architectural differences between these resin types. This heterogeneity in turn influences the receding compliance for the E_r measurements during the nanoindentation [42].

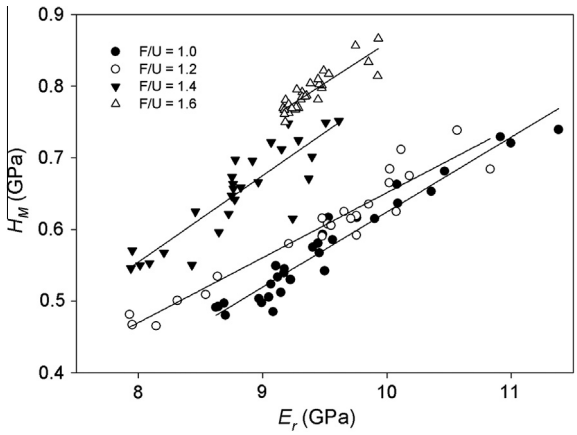

Fig. 8. Relationship between H_M and E_r of cured UF resin films as a function of F/U mole ratio.

The relationship between H_M and E_r obtained by the nanoindentation method is shown in Fig. 8. The results clearly indicate that the H_M and E_r values have positive linear relationships even though there is a relatively large variation in the measurements, which can be attributed to heterogeneity of the surface compositions/textures of samples, depending on the F/U mole ratio. In other words, the F/U mole ratio of cured UF resins has a profound impact on H_M and E_r measurements.

4. Conclusions

This study investigated hardness of cured UF resins with different F/U mole ratios by the nanoindentation method, comparing with the traditional Brinell hardness (H_B). The H_B of cured UF resin films with different F/U mole ratios was determined by exposing them to different post-curing temperatures. The nanoindentation provided Meyer hardness (H_M) and reduced modulus (E_r) that has been used to obtain the sample elastic modulus (E_s) of cured UF resins by calculation from the nanoindentation. The following conclusions were drawn from this study:

1. As the F/U mole ratio increased, the H_B increased continuously. The H_B values also increased with an increase in the post-cure temperature. The H_M value also showed a similar trend as a function of F/U mole ratio.
2. However, the trend for E_r and E_s was not as consistent as for H_M and H_B. Both H_M and E_r showed much greater variation in the coefficient of variation (COV) with the cured UF resins at lower F/U mole ratios (1.2 and 1.0), indicating a heterogeneous composition.
3. Linear relationships between H_M and E_r indicate that heterogeneity of the surface composition of samples contribute greatly to the variations recorded. Greater variability in cured UF resins with low F/U mole ratios is likely to be due to their greater compositional/textural heterogeneity, resulting likely from higher frequency of globular particles and the presence of crystalline domains inter-dispersed within non-crystalline phases.

Acknowledgements

This work was supported by the Basic Science Research Program through the National Research Foundation (NRF) of Korea funded by the Ministry of Education, Science and Technology (2011-0022112). This work was also financially supported by the Ministry of Education Science and Technology (MEST) and The Korean Federation of Science and Technology Societies (KOFST).

References

[1] Johns WE, Dunker AK. In: Meyer B, Andrews BAK, Reinhardt RM, editors. Formaldehyde release from wood products. The American Chemical Society; 1986. p. 76–86.
[2] Myers GE. Wood Sci 1982;15:127–38.
[3] Myers GE. For Prod J 1983;33:27–37.
[4] Myers GE. In: Meyer B, Andrews B, Reinhardt RM, editors. Formaldehyde release from wood products. American Chemical Society; 1986. p. 87–106.
[5] Marutzky R. In: Pizzi A, editor. Wood adhesives: chemistry and technology, vol. 2. Marcel Dekker Inc.; 1986. p. 307–87.
[6] Park BD, Lee SM, Roh JK. Eur J Wood Prod 2009;67:121–3.
[7] Pizzi A, Lipschitz L, Valenzuela J. Holzforschung 1994;48:254–61.
[8] Hse CY, Xia ZY, Tomita B. Holzforschung 1994;48:527–34.
[9] Gu JY, Higuchi M, Morita M, Hse CY. Mokkuzai Gakkaishi 1996;42:149–56.
[10] Myers GE. For Prod J 1984;34:35–41.
[11] Park B-D, Kim JW. J Appl Polym Sci 2008;108:2045–51.
[12] Park BD, Kang EC, Park JY. J Appl Polym Sci 2006;101:1787–92.
[13] Myers GE. In: Christiansens AW, Gillespie R, Myers GE, River BH, editors. Proceedings of wood adhesives in status and needs. For. Prod. Res. Society; 1986. p. 119–56.
[14] Tohmura S, Hse CY, Higuchi M. J Wood Sci 2000;46:303–9.
[15] Robitschek R, Christensen RL. For Prod J 1976;26:43–6.
[16] Park BD, Jeong HW. In: Proc. of 2009 International Conference on Wood Adhesives, Harveys Resort Hotel & Casino, Lake Tahoe, Nevada, USA, September 28–30, 2009.
[17] Poole Jr CP, Owens FJ. Introduction to nanotechnology. Hoboken (New Jersey): John Wiley & Sons, Inc.; 2003. p. 35–71.
[18] Oliver WC, Pharr GM. J Mater Res 1992;7:1564–83.
[19] VanLandingham MR, Villarrubia JS, Myers GF. Polym Preprint 2000;41:1412–3.
[20] VanLandingham MR, Villarrubia JS, Guthrie WF, Myers GF. Macromol Symp 2001;167:14–43.
[21] Wang M, Liechti KM, White JM, Winter RM. J Mech Phys Solids 2004;52:2329–54.
[22] Jakes JE, Lakes RS, Stone DS. J Mater Res 2012;27:464–74.
[23] Jakes JE, Lakes RS, Stone DS. J Mater Res 2012;27:475–84.
[24] Gouldstone A, Koh H-J, Zeng K-Y, Giannakopoulos AE, Suresh S. Acta Mater 2000;48:2277–95.
[25] Konnerth J, Jager A, Eberhardsteiner J, Muller U, Gindl W. J Appl Polym Sci 2006;102:1234–9.
[26] Wimmer R, Lucas N. J Int Assoc Wood Anatomy 1997;18:77–88.
[27] Wimmer R, Lucas N, Tsui TY, Oliver WC. Wood Sci Technol 1997;31:131–41.
[28] Gindl W, Gupta HS, Grünwald G. Can J Bot 2002;80:1029–33.
[29] Gindl W, Schöberl T. Composites Part A 2004;35:1345–9.
[30] Yu Y, Fei B, Zhang B, Yu X. Wood Fiber Sci 2007;39:527–35.
[31] Konnerth J, Valla A, Gindl W. Appl Phys A 2007;88:371–5.
[32] Jakes JE, Stone DS, Frihart CR. In: Proceedings of 31st Annual Meeting of the Adhesion Society, Austin, TX, USA, Feb 17–20, 2008, The Adhesion Society Inc, Blacksburg, VA, Feb. 17–20, 2008a. p. 247–9.
[33] Obersriebnig M, Veigel S, Gindle-Altmuter W, Konnerth J. Holzforschung 2012;66:781–7.
[34] Jiang Z, Yu Y, Qin D, Wang G, Zhang B, Fu Y. Holzforschung 2006;60:698–701.
[35] Vlad-Cristea M, Riedl B, Blanchet P, Jimenez-Pique E. Eur Polym J 2012;48:441–53.
[36] Park B-D, Jeong H-W. J Korean Wood Sci Technol 2011;39:179–86.
[37] Park B-D, Jeong H-W, Lee S-M. J Appl Polym Sci 2011;120:1475–82.
[38] Park B-D, Jeong H-W. Int J Adhes Adhes 2011;31:524–9.
[39] Stuligross J, Kousky JA. J Adhes 1985;18:281–99.
[40] Despres A, Pizzi A. J Appl Polym Sci 2006;100:1406–12.
[41] Park B-D, Causin V. Eur Polym J 2013;49:532–7.
[42] Jakes JE, Frihart CR, Beecher JF, Moon RJ, Stone DS. J Mater Res 2008;23:1113–27.